# Autotuning of Resonant Magnetic Induction Communications

Hirsa Kia and Krishna Kant
Temple University

***Abstract*—**

***Index Terms*—Magnetic Induction Communications, Autotuning, Resonance, Q-factor**

## I. Introduction

Smart sensing and short-range wireless communications form the bedrock for building sophisticated IoT based automation services for close-range monitoring of various types of activities. Radio frequency (RF) based communications (e.g., Bluetooth, WiFi) are well established and work extremely well in open, uncluttered environments, and are thus the technology of choice for longer range communications through the air. However, increasingly the communications needs involve environments with characteristics that make RF communications difficult – these include presence of aqueous or plant/animal tissue media which cause high signal absorption, metallic clutter that causes diffraction or shielding of the signals, or underground operation that results in an extremely complex communications channel. Reducing absorption by choosing lower frequencies helps in attenuation [1], [2], but needs bigger antennas, which introduces the problem of undesirable size and potentially severe interference with nearby radios. Also, the power consumption of RF radios is generally quite high. When localization is important, narrow-band RF technologies only provide an accuracy of a few meters, which may be inadequate [3].

Ultrasound communication (USC) is a well established non-RF technology that works well in aqueous and underground media, but requires larger size radios and higher power consumption, but still cannot operate in a cluttered environment. Visible light communication (VLC) is an excellent technology for line-of-sight communications through transparent media, but its performance deteriorates rapidly in the presence of obstacles.

Another well-known short-range non-RF technology is based on the principle of resonant inductive coupling (RIC) between two matched coils, each forming an LC circuit with the same resonance frequency. Magnetic resonance communication (MRC) modulates the magnetic field and forms the basis for near field communications (NFC). Such communication can be made purely magnetic by blocking the electric field (e.g., via an Aluminium foil) and therefore will not suffer from the usual fading and diffraction associated with the electric field. Due to these advantages, MRC has been studied for some RF-challenged environments such as underwater [4], underground [5], and Body Area Networks [**?**], and some commercial products are available, such as audio headphones by NXP [6] and RuBee MRC tags useful in product labeling [7].

We have examined MRC in two contexts; (a) monitoring the quality deterioration of fresh-foods while they are being transported or stored during transit [8], [9], and (b) Human Body Communications (HBC) [10]–[12]. Our work has shown that MI works better than other HBC technologies such as Capacitive or Galvanic coupling [12] and comparable to ultrasound [13]. Other researchers have also examined MI and other HBC technologies [14], [15]. We also found that MRC is also very robust against variations that one would expect in on/in-body environment such as movement, posture, clothing, person to person variations (e.g., build, weight, etc.) [12]. We note that in contrast MRC antennas have been reported to be very sensitive to misalignments [16] and require proper acoustic impedance matching [17].

In the context of HBC, an interesting emerging application of MRC is communications among the nodes of (usually small) networks some of which may be inside the body, while some are on-body. The primary use case for these is the management of chronic diseases that continue to rise rapidly throughout the world due to the rapidly aging population in developed countries [18], [19] and increasing air, water, and food pollution in developing countries [20]. In the US, more than 50% of older adults $\geq$ 3 chronic conditions [18]. According to the US CDC, chronic diseases account for nearly 75% of aggregate healthcare spending, and their treatment accounts for 96% of Medicare costs and 83% of Medicaid costs [21], [22]. Management of chronic diseases, often requires collecting relevant signals (e.g., nerve conduction, muscle activity, blood flow, etc.) from multiple points and their fusion to determine the actuation (drug or electric stimulation delivery). For example, overactive bladder control ideally involves a spinal cord neuro-modulator based on the bladder pressure monitoring by an implantable pressure sensor and the urine volume monitoring by micro-electrode-mediated neural recording [23]–[25]. Thus the need for an intra-body network of nodes, communicating via MRC is one of the important scenarios.

A crucial aspect of such intrabody networks is the serious limitations that they face. The nodes should be as small as possible to avoid tissue damage, should last for as long as they are needed (or the lifetime of the patient), and should not require any adjustments/changes. Thus, the wireless power transfer (WPT) to the nodes (along with supercapacitors to hold the charge) is a much more desirable solution than

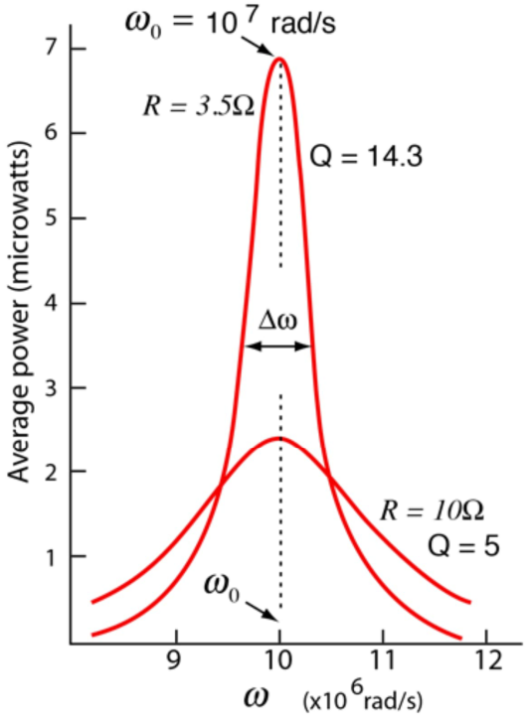


Fig. 1: Power transfer vs. Frequency in Resonant RLC Circuit

batteries. The energy transfer could occur either from an energy harvesting node inside the body (e.g., close to the heart or lungs) or supplied from a battery-operated on-body device such as a smart watch. An efficient WPT mechanism is crucial to ensure that the nodes can receive adequate energy supply. Note that even a small 20db path-loss through the body would reduce 1 mW transmitted power to only $10\mu$W on the receiver side. Put another way, 99% of the transmitted power will be wasted or absorbed by the tissue.

Given this backdrop, it is crucial to make MRC based communication and power transfer highly efficient, and keep it so over very long periods of time (e.g., 10's of years) without need for any physical access for the purposes of tuning the circuits. This is the topic that we address in this paper and propose an autotuning scheme to ensure the highest possible energy transfer without any manual intervention.

## II. Q Factor and Autotuning

MRC works by energy transfer between a transmit and a receive coil separated by the desired communication distance. Each coil has certain inductance $L$ and connected to a capacitor $C$ in series or in parallel, plus a resistor in series to control the current. At any angular frequency $\omega = 1\pi f$, such a circuit has capacitive and inductive reactances, denoted $X_C$ and $X_L$ respectively, given by $X_C = -1/(j\omega)$ and $X_L = j\omega$. The total impedance of a series RLC circuit is given by

$$Z = R + j\left(X_L - X_c\right) = R + j\left(\omega L - \frac{1}{\omega C}\right) \tag{1}$$

When $X_L > X_C$ the circuit is *inductive*, whereas $X_C > X_L$ makes the circuit *capacitive*. Electrical resonance occurs in an AC circuit when the inductive and capacitive reactance are equal, i.e.,

$$X_L = X_c, \quad \Longrightarrow \omega_r L = \frac{1}{\omega_r C}, \quad \Longrightarrow \omega_r = \frac{1}{\sqrt{LC}} \tag{2}$$

In resonant condition, the impedance of the circuit becomes purely resistive, i.e. $Z = R$.

An important performance indicator of an RLC circuit is the *quality factor* $Q$, defined as the ratio of the energy stored in the circuit to the energy dissipated by the circuit [26], [27]. It is merely the ratio of reactance and resistance, and is given by $Q = 1/\omega_r RC)$.

$$\begin{aligned} Q &= \frac{\text{Energy stored in the circuit per cycle}}{\text{Energy dissipated by the circuit per cycle}} \\ &= \frac{\text{Reactance}}{\text{Resistance}} = \frac{X_L \text{ (or } \mathrm{X_C})}{R} = \frac{\omega_r L}{R} = \frac{1}{R\omega_r C} \end{aligned} \tag{3}$$

The quality factor mainly indicates how efficiently inductors and capacitors in the circuit transfer their energy from the source to the load. The quality factor is also defined as the frequency-to-bandwidth ratio of the resonator, i.e.

$$Q = \frac{f_r}{\Delta f} = \frac{\omega_r}{\Delta\omega} \tag{4}$$

where $\Delta f$ is the resonance width, i.e. the bandwidth over which the power is greater than half the power at the resonant frequency $\Delta\omega$ is the corresponding angular half-power bandwidth(See Fig. 1). From equation(3)-(4) we can observe that the bandwidth of the RLC circuit can be controlled by the resistance only, keeping all the other components same.

The transmit coil can transfer energy to the receive coil because of the mutual inductance between the two coils, denoted $M$. Thus a time varying voltage $V_1$ (and corresponding current $I_1$) in the transmit coil induces a current $I_2$ in the receiving coil. If the resistor, inductor, and capacitor values of the two coils are $(R_1, L_1, C_1)$ and $(R_2, L_2, C_2)$ respectively, then from Kirchoff's laws, it is easy to conclude that $I_2 = -\frac{j\omega_r M}{R_2} I_1$. Thus if the transmit data is modulated on the magnetic flux, then the receiver can receive and demodulate the signal. The effectiveness of the mutual coupling is measured by the *coupling coefficient* $\kappa$, which can be estimated as

$$\kappa = \frac{M}{\sqrt{L_1 L_2}} \tag{5}$$

If $P_1$ and $P_2$ are the transmitted and received power respectively, then the power transfer ratio is given by [27]

$$\frac{P_2}{P_1} = \frac{\omega_r^2 M^2 R_1 R_2}{R_1^2 R_2^2} = \kappa^2 Q_1.Q_2 \tag{6}$$

where $Q_1$ and $Q_2$ are the quality factors of the transmit and receive coils respectively. Thus, the power transfer is proportional to the coupling coefficient and the quality factors of the transceiver coils.

It is clear that to maximize energy transfer, both $Q_1$ and $Q_2$ should be as high as possible. Unfortunately, a high $Q$ value results in a much sharper peak in the resonance curve as shown in Fig. 1. The key problem with the sharp peak is its stability, since a slight drift in the parameters or load variations can change the resonance frequency enough to substantially lower the transfer efficiency. In this paper we devise an autotuning mechanism to ensure that any drift is compensated for and thus the energy transfer stays near its peak.

In general, there could be multiple reasons for drift, some significant, some not. For example, the drift in the capacitance due to aging and temperature variations depends on the type of capacitor used. For small capacitances relevant for the resonant LC tank, a class 1 CoG capacitor is ideal, and its aging and temperature related variables are generally quite small or negligible (see https://www.electronics-notes.com/articles/electronic_components/capacitors/ceramic-dielectric-types-c0g-x7r-z5u-y5v.php). However, the mounting of the capacitor on the circuit board and the solder can experience significant changes over time, particularly at higher temperatures [28]. The change could eventually lead to failures; however, our focus here is not failure, but the drift in properties that occurs over a long period much before outright failure.

In addition to the potential drift in the resonance circuit itself, there are other changes whose impact could be perturb the resonance significantly. One source of perturbation is the movement of the transmit or receive coil while it is deployed in the patient. Depending on the location, slight movements and orientation changes occur as the body muscles move. These movements would also change the parasitic capacitance contributed by the the body and its contact with the coils. The net effect of these variation is the change in the resonance circuit parameters and thereby a drop in power delivered to the load.

### A. Related Work

The problem of "detuning" of resonant circuits due to various impacts has been well recognized and studied in the context of wireless power transfer (WPT). Note that our problem involves integrated WPT and communication which places certain restriction as compared with pure WPT environment. The main techniques as described below.

The most direct compensation method is to introduce a switchable capacitor/inductor matrix to compensate for the capacitance drift. However, the solutions tend to be rather heavy duty and intended for large power transfer situations. For example, Si et. al. [29] consider power transfer to pacemaker from outside and describe a way of changing frequency of operation to regular power transfer. It includes both capacitor switching and frequency switching to control power transfer. Lim et al. [**?**] introduce a self-adaptive capacitor matrix with automated searching for configuration with changing distance between transmit and receive coils.

Another method is to adjust the capacitance via pulse-width modulation (PWM) of the input signal in order to control how much chance the capacitor gets to charge/discharge in each cycle, which effectively changes its capacitance. Porto et al. [30] do this by using an amplifier, and a double-sided version is discussed in [31]. However, such complexity in unwarranted since voltage controlled capacitors, many built in with push-pull circuit are readily available. Furthermore, PWM can interfere with the communication in the integrated power transfer and communications mechanism that we are interested in.

Switching the operating frequency to always correspond to the resonant frequency is a popular method explored in several papers. For example, a self-oscillating switching technique was used in [32]. For our application, frequency switching is undesirable as it is complex and requires the receiver to re-latch to the change frequency to enable proper communication.

Another method is to control the phase shift on the receive side by using the semiactive rectifier (SAR) where the trigger modes of the driving signals are altered to achieve matching of the load resistance or reactance. Mai, et.al. [33] use both pulse width and the phase shift angle control to provide matching for both the drift and load resistance variations. In our context the rectification will work only for WPT, not communications.

## III. Capacitive Tuning

### A. Circuit Design

Two RLC circuits with magnetic flux coupling were designed. The main criteria was to have an efficient energy transfer between the two circuits in a specific frequency (13.56 MHz). The values for resistance, inductance and capacitance can be obtained from the resonance frequency and $Q$ factor. According to [34], to have an optimal energy transfer, the transfer coefficient $k_{mrc}$ needs to equal to $\frac{1}{\sqrt{Q_r \cdot Q_t}}$. Here it is assumed that is actually the case in our simulations.

| | |
|---|---|
| $L$ | 9.27 $\mu$ H |
| $C$ | 14.86 pf |
| $R$ | 50 $\Omega$ |
| $k_{mrc}$ | 0.063 |

TABLE I: Circuit parameters

To simulate circuits, LTspice®software was used. LTspice®is a powerful, fast, and free SPICE simulator software, schematic capture and waveform viewer with enhancements and models for improving the simulation of analog circuits. Its graphical schematic capture interface allows you to probe schematics and produce simulation results, which can be explored further through the built-in waveform viewer [35].

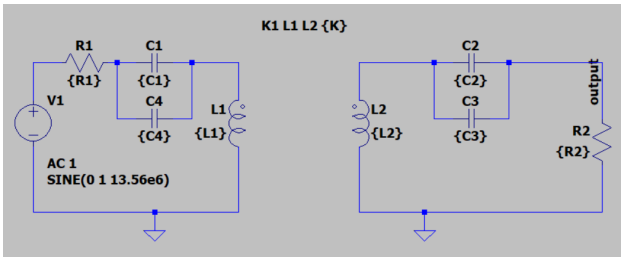


Fig. 2: Circuit in LTspice

Using LTspice®, the current, voltage and power were calculated in the following table:

| | |
|---|---|
| $i_t$ | 7.041 mA |
| $v_t$ | 703 mV |
| $i_r$ | 6.865 mA |
| $v_r$ | 343 mV |
| Efficiency | 47.57 % |

TABLE II: Circuit performance

Subscripts t and r denote transmitter and receiver, respectively.

### B. On-Body Experiments

As it was seen in equation 6, the efficiency of transmission would depend on the q-factors of transmitter and receiver and the coupling factor of the medium. In a complex medium such as human body, it would be naive to assume that the coupling factor would only have a constant value. We conducted a couple of simple experiments, in which we used the transmitter and receiver of a pair of matching circuits on skin to measure how the efficiency would change. Two matching circuits were built, specifications of which are discussed in the next subsection. The circuit is built according to the circuit in [12]. Then the two coils (transmitter and receiver) are be placed on the left hand arm, 15 centimeters apart.

*1) Skin Temperature:* First experiment was with skin temperature, in which we increased/decreased body temperature and measure the efficiency. A rubber bottle was used as the heating/cooling agent. The bottle then was placed on the arm, between the two sensors and removed after 2 minutes. The experiments were done by 4 different temperatures, $10°$, $15°$, $27°$, $35°$ and $40°$ Celcius. As it can be seen in figure 3, there is less than 1.78 dB loss between maximum and minimum measured dB loss and there is no apparent correlation between the temperature and efficiency.

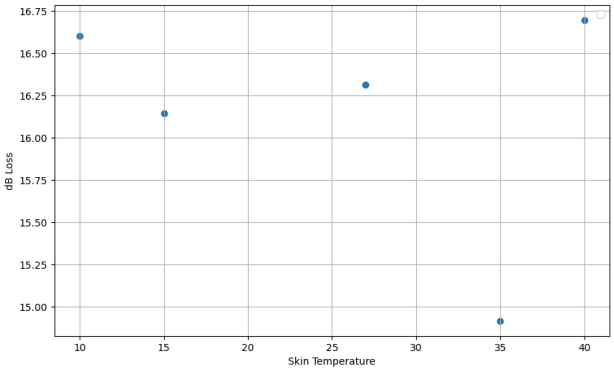


Fig. 3: dB Loss vs. Skin Temperature

*2) Blood pressure:* Second experiment was with blood pressure, in which we measured the blood pressure (both Diastolic and Systolic) and efficiency. The measurements were done in different times of the day and after different activities, in order to get a range of numbers covered for BP. As it can be seen in the figure 4, it changes rather drastically. Although our experiments may not present a direct correlation between the two, what we can see is that it is a highly volatile and complex transmission medium that needs maintenance in order to establish a stable and efficient connection Bearing in mind how complex and unstable the transmission can be, we proceed to the next section to propose the controller.

### C. Control Scheme

Here, two main scenarios are investigated: First, the drift is modelled as a trapezoid, which starts and ends in both transmitter and receiver. Second, the drift is modelled as a saturating ramp, which starts slowly but never ends and happens in both transmitter and receiver.

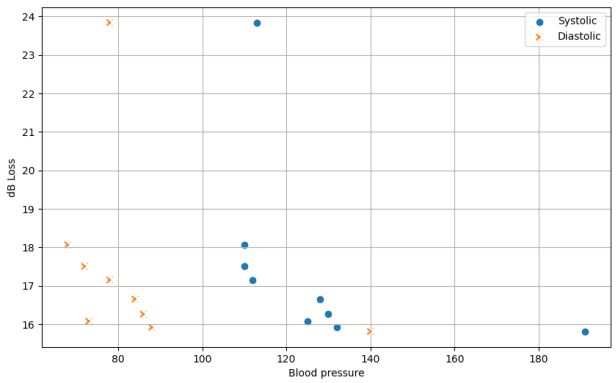


Fig. 4: dB Loss vs. Blood Pressure

Due to the nature of the problem, which is to be as efficient as possible in generating the control signals, a very simple scheme was implemented. As it is shown in the 5, the current in the receiver circuit goes downhill whenever the two circuits do not match in resonant frequency. So the key part of the controller is that it should find out which part of the slope we are on. The controller only observes the current and whenever the current is not at its maximum, it activates. Upon activation, it increases and decreases the capacitance, measuring the current after each action. When increased/decreased, if the current is higher than the current measured before activation, it keeps increasing/decreasing the capacitance. Otherwise, it changes direction, meaning if it was increasing the capacitance until now, it starts decreasing the capacitance, and vice versa, as it is shown in Algorithm 1. The interest in controlling capacitors matching is due to the fact that it has a very small value, so there is a higher probability of parasitic capacitance interfering with the designed capacitance. To design the controller, a truth table is constructed for behavior of controller. To do so, the following equations are defined:

$$\delta = Sign(C_{t-1} - C_{t-2}) \tag{7}$$

$$\Delta_1 = Sign(I_t - I_{t-1}) \tag{8}$$

$$\Delta_2 = Sign(I_{t-1} - I_{t-2}) \tag{9}$$

Controller truth table is shown in Tables III and IV, as they represent two different scenarios. To clarify, the action means the direction of the step (or sign of the step) that the controller should decide to take. In the figure 6.b, the orange line is used to show the optimal value of capacitance. The controller acts upon in every scenario according to three data flow it receives, current and action from one time sample before, current and action from two time sample before and time.

| Action | -1 | -1 | -1 | -1 |
|---|---|---|---|---|
| $\Delta_1$ | +1 | -1 | -1 | +1 |
| $\Delta_2$ | +1 | -1 | -1 | +1 |
| $\delta$ | +1 | -1 | +1 | -1 |

TABLE III: Controller Truth Table 1

At first, we investigated the one-side control scheme, in which only transmitter would have the controller implemented on it, meaning that whether the drift happens on the transmit or receive side, the controller would only be able to tune the

**Algorithm 1** Controller Pseudocode

**Observations:**
$I_t$ := Receiver Current at time t
$I_{t-1}$ := Receiver Current at time t-1
$I_{t-2}$ := Receiver Current at time t-2
$C_{t-1}$ := Capacitance at time t-1
$C_{t-2}$ := Capacitance at time t-2

**Parameters:**
$W'$ := Initialization weight
$W$ := Weight
$\epsilon$ := Threshold
$\Delta$ := Step size
$\alpha$ := Control Action
$\delta = Sign(C_{t-1} - C_{t-2})$
$\Delta_1 = Sign(I_t - I_{t-1})$
$\Delta_2 = Sign(I_{t-1} - I_{t-2})$

**if** NOT Controller's Turn **then**
  $C_t \leftarrow C_{t-1}$
**else**
  **if** $|I_t - I_{ref}| < \epsilon$ **then**
    $C_t \leftarrow C_{t-1}$
  **else**
    **if** t=1 (First round) **then** *Initialization*
      $C_t \leftarrow C_{t-1} + W'\Delta$
    **else**
      $C_t \leftarrow C_{t-1} + W^t \cdot \alpha \cdot \Delta$

| Action | +1 | +1 | +1 | +1 |
|---|---|---|---|---|
| $\Delta_1$ | +1 | -1 | -1 | +1 |
| $\Delta_2$ | +1 | -1 | -1 | +1 |
| $\delta$ | -1 | +1 | -1 | +1 |

TABLE IV: Controller Truth Table 2

circuit on the transmit side. As you can see in Table V, we implemented this scenario with 5% drift on receiver side, and using the controller, we are only able to recover 1%.

| 5(%) increase | $I_{out}$(mA) | $P_{out}$(mW) | Eff(%) | C(pf) |
|---|---|---|---|---|
| Before control | 6.62 | 2.19 | 36.3 | 7.43 |
| After control | 6.84 | 2.34 | 37.4 | 7.77 |
| Optimal values | 6.85 | 2.35 | 37.5 | 7.82 |

TABLE V: Performance of Transmitter side controller in 5% increase drift on Receiver side

What it means is that using one-side control scheme, cannot recover the drift that might happen on the side missing the controller. This is why we moved to having the controllers on both receive and transmit sides.

Since we have two controllers, on both transmitter and receiver side, we schedule the operation of each controller. What it means is, we give each controller a time interval to act, in this interval the controller figures out whether it should turn on and the direction it needs to act. In each interval, the controller starts by checking the current. If it is less than the reference by more than the amount of $\epsilon$, the controller's first action is to implement an initial increase in capacitor, using

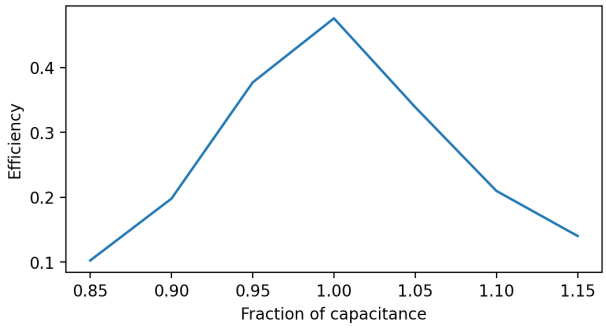


(a) Efficiency

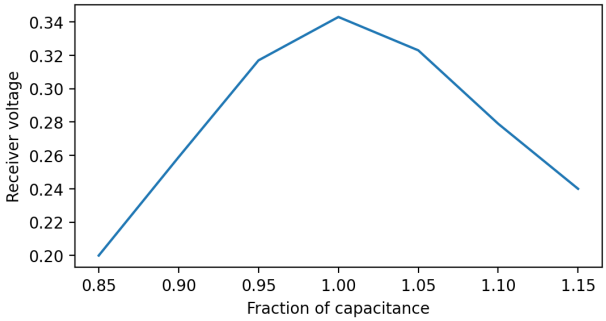


(b) Receiver Voltage

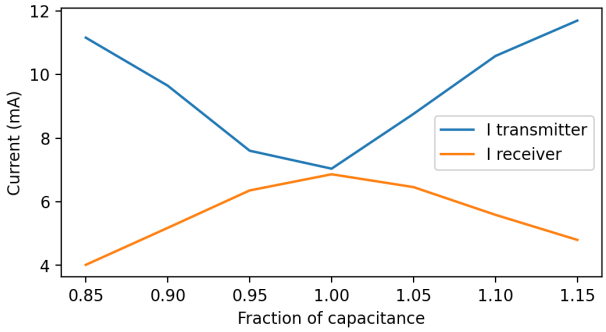


(c) Transmitter and Receiver Currents

Fig. 5: Receiver Circuit Perturbed

this initialization the controller figures out which direction to select using the truth table shown in figure 6. We also give a decreasing weight to each change the controller wants to implement in capacitance. So the controller output would look like as below:

$$Controller\ Sequence = \left\{C + W^t \cdot \alpha \cdot \Delta\right\}_{t=1}^{N} \quad (10)$$

In equation 10, $\alpha$ denotes the action, $\delta$ represents the step size and W is the weight which is a number smaller than 1.

| 5(%) increase | $I_{out}$ (mA) | $P_{out}$ (mW) | Eff (%) | C (pf) | Recovery (%) |
|---|---|---|---|---|---|
| Before control | 6.494 | 2.108 | 35.53 | 7.43 | |
| After control | 6.925 | 2.398 | 46.97 | 7.77 | 91.74 |
| Optimal values | 6.927 | 2.4 | 48 | 7.82 | 100 |

TABLE VI: Performance of controller in 5% increase drift

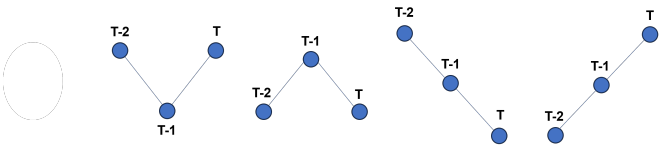


(a) Current Trajectory

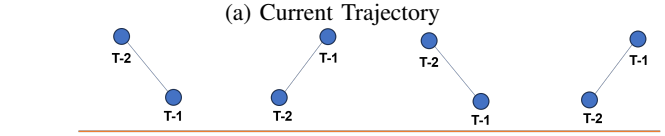


| | | | | |
|---|---|---|---|---|
| δ | -1 | +1 | -1 | +1 |
| Action | -1 | -1 | -1 | -1 |

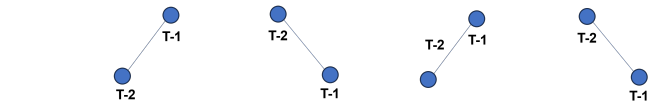


| | | | | |
|---|---|---|---|---|
| δ | +1 | -1 | +1 | -1 |
| Action | +1 | +1 | +1 | +1 |

(b) Capacitance Trajectory

Fig. 6: Controller Truth Table

### D. Controller Performance

To demonstrate the performance of the proposed controller, worst scenario of drifting was needed to be selected. There are two major categories which are that the drifting in transmit and receive side happen in the same direction (increasing or decreasing) or in opposite directions. As it is expected, if the drifting happen in the same direction, they would reach a new resonant state, which is not in the working frequency but at least some of the loss is compensated this way. Worst case is that the two capacitances would drift in opposite directions.

**First Scenario**: The drifting has been modelled by a trapezoid with height equal to 5 % of capacitance. The proposed controller adapts to the drift according to the step size. It recovers over 96 % of the maximum power and over 98 % of the maximum current and voltage. Since the controller is using a very simple and energy efficient control strategy, it always settles in the range of 4 % of the designed capacitance. As for the efficiency, at worst it experiences 44% efficiency.

**Second Scenario**: The drifting has been modelled by a saturating ramp with max equal to 5% of capacitance. As it is shown in Figure 8, The proposed controller adapts to the drift according to the step size. It recovers over 98% of the maximum power and over 99% of the maximum current and voltage. Since the controller is using a very simple and energy efficient control strategy, it always settles in the range of 3% of the designed capacitance. As for the efficiency, at worst it experiences 48% efficiency when converged. The controllers manage to find a new resonant frequency without sacrificing so much efficiency and power, very quickly.

## IV. Discussions

- The sharp drops in current and power are due to the fact that drift, pushes us off the optimum rather sharply. However, the controller is able to bring us back to optimal (near optimal, to be precise) value. As it is observed in second scenario, we do not experience such drops in current and power because we are able to compensate for the slow changes.
- The controller can be very fast on balancing the capacitors. The speed is dependent on the activation value $\epsilon$ and step size. Of course, the speed would play as an adversary to the energy efficiency of the controller and the trade off can be studied before implementation.
- Since the controllers act on both transmitter and receiver sides and they do not share their actions, the capacitance value does not settle on a single value (although its change is bounded). Interestingly, the efficiency keeps being high, due to the tracking behavior of controllers. They both keep tracking the optimal value and the other controllers value, hence what we achieve might not be the exact optimal value, but the near optimal value and more importantly, resonance in frequency.
- As we have shown it in the cartoon provided in figure 9, what happens is, essentially, some body properties change over time (creating a time series) which would in return change the properties of the magnetic communications (improving or worsening it) in circuit level. Controller would only see the circuit level (received current and power are the observations of the controller). Hence, no matter how complex the model between the body properties and circuit variables are, it would not matter to the controller at all. At some point, one might be able to obtain a model that would translate body properties to circuit variables, which in turn can make the controller have a more efficient connection.
- As the

## V. Conclusions

## References

[1] R. Jedermann *et al.*, "Communication techniques and challenges for wireless food quality monitoring," *Philosophical Transactions of the Royal Society*, vol. 372, no. 2017, p. 20130304, 2014.

[2] F. A. Khan, "Sub-gigahertz wireless sensors for monitoring of food transportation," Master's thesis, University Bremen, 2015.

[3] H. Liu, H. Darabi, P. P. Banerjee, and J. Liu, "Survey of wireless indoor positioning techniques and systems," *IEEE Trans. Systems, Man, and Cybernetics, Part C*, vol. 37, no. 6, pp. 1067–1080, 2007.

[4] I. F. Akyildiz *et al.*, "Realizing underwater communication through magnetic induction," *IEEE Communications Magazine*, vol. 53, no. 11, pp. 42–48, 2015.

[5] Z. Sun *et al.*, "Magnetic induction communications for wireless underground sensor networks," *IEEE Transactions on Antennas and Propagation*, vol. 58, no. 7, pp. 2426–2435, 2010.

[6] "NXP Introduces Ultra-low Power Radio Transceiver Enabling Wireless Earbuds," http://www.everythingrf.com/News/details/1399-nxp-introduces-ultra-low-power-radio-transceiver-enabling-wireless-earbuds.

[7] http://ru-bee.com/.

[8] A. Pal and K. Kant, "Nfmi: Near field magnetic induction basedcommunication," *Elsevier Computer Networks*, Nov 2020.

[9] ——, "Magloc: A magnetic induction basedcommunication scheme for fresh food logistics," *Elsevier IoT Journal*, vol. 19, Aug 2022.

[10] R. Gulati, A. Pal, and K. Kant, "Experimental evaluation of a near-field magnetic induction based communication system," *Wireless Communications and Networking Conference, Marrakech, Morroco*, April 2019.

[11] R. K. Gulati, S. Islam, A. Pal, K. Kant, and A. Kim, "Characterization of magnetic communication through human body," *IEEE Consumer Communications and Networking Conference (CCNC)*, pp. 563–568, Jan 2022.

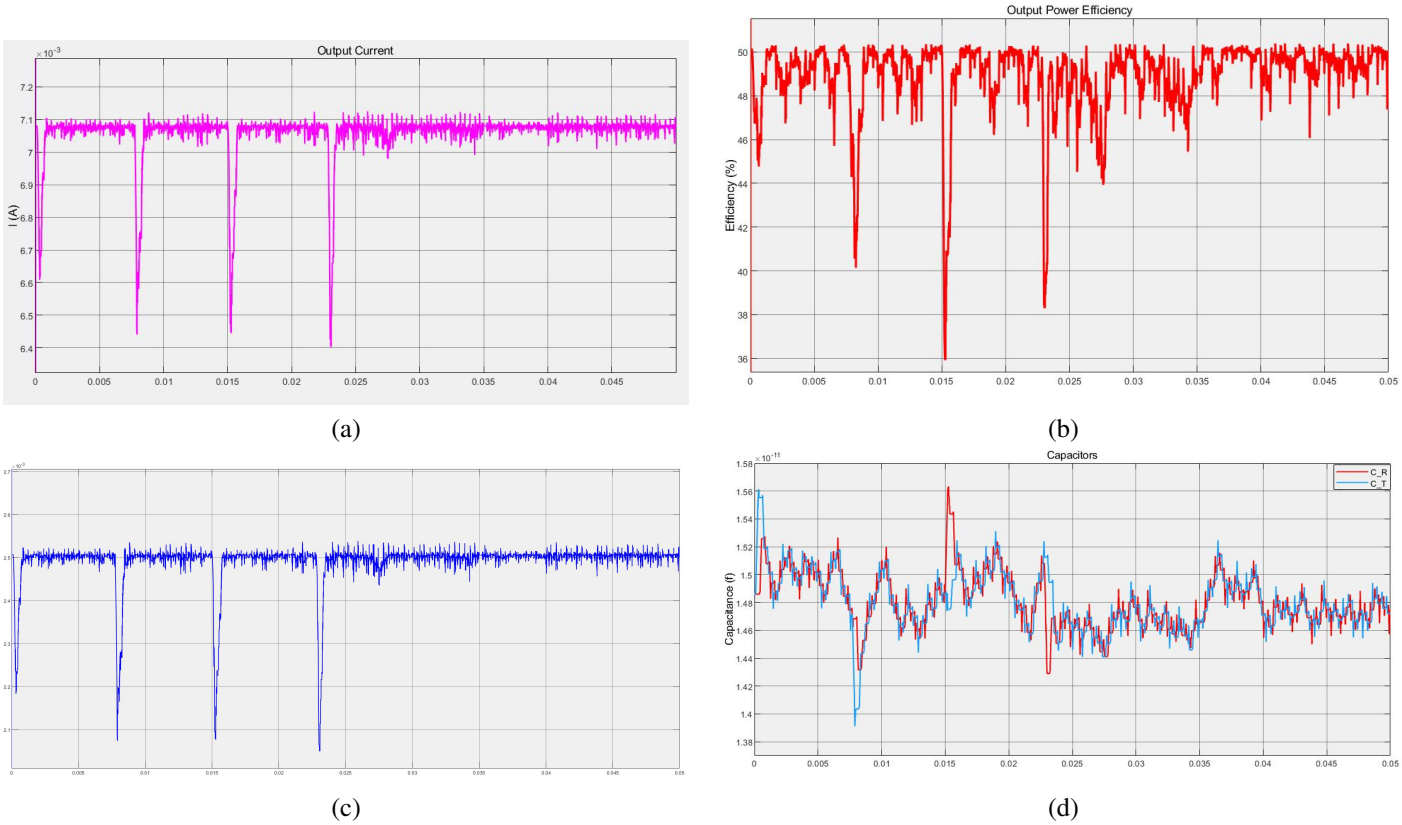


(a) (b) (c) (d)

Fig. 7: First Scenario Controller Performance: a. Output current, b. Efficiency, c. Output power, d. Receiver and transmitter capacitances


[12] S. Islam, R. K. Gulati, M. Domic, A. Pal, K. Kant, and A. Kim, "Performance evaluation of magnetic resonance coupling method for intra-body network (ibnet)," *IEEE Transactions on Biomedical Engineering*, vol. 69, no. 6, pp. 1901–1908, June 2022.

[13] R. Gulati, K. Kant, and A. Pal, "Ultrasonic vs. magnetic resonance communication for mixed wearable and implanted devices," *Proc. of IEEE International Conf. on Communications (ICC)*, pp. 5304–5309, May 2022.

[14] W. J. Tomlinson, S. Banou, C. Yu, M. Stojanovic, and K. R. Chowdhury, "Comprehensive survey of galvanic coupling and alternative intra-body communication technologies," *IEEE Communications Surveys & Tutorials*, vol. 21, no. 2, pp. 1145–1164, 2018.

[15] J. Park and P. P. Mercier, "Magnetic human body communication," in *2015 37th Annual International Conference of the IEEE Engineering in Medicine and Biology Society (EMBC)*. IEEE, 2015, pp. 1841–1844.

[16] A. Ibrahim, M. Meng, and M. Kiani, "A comprehensive comparative study on inductive and ultrasonic wireless power transmission to biomedical implants," *IEEE sensors journal*, vol. 18, no. 9, pp. 3813–3826, 2018.

[17] T. C. Chang, M. J. Weber, M. L. Wang, J. Charthad, B. P. T. Khuri-Yakub, and A. Arbabian, "Design of Tunable Ultrasonic Receivers for Efficient Powering of Implantable Medical Devices With Reconfigurable Power Loads," *IEEE Transactions on Ultrasonics, Ferroelectrics, and Frequency Control*, vol. 63, no. 10, pp. 1554–1562, Oct. 2016. [Online]. Available: http://ieeexplore.ieee.org/document/7562528/

[18] A. Tinker, "How to improve patient outcomes for chronic diseases and comorbidities," http://www.healthcatalyst.com/wp-content/uploads/2014/04/How-to-Improve-Patient-Outcomes.pdf, 2017.

[19] W. H. Organization, "World report on aging," https://apps.who.int/iris/bitstream/handle/10665/186463/9789240694811_eng.pdf, 2015.

[20] G. Yang, L. Xie, M. Mäntysalo, X. Zhou, Z. Pang, L. Da Xu, S. Kao-Walter, Q. Chen, and L.-R. Zheng, "A health-iot platform based on the integration of intelligent packaging, unobtrusive bio-sensor, and intelligent medicine box," *IEEE transactions on industrial informatics*, vol. 10, no. 4, pp. 2180–2191, 2014.

[21] L. P. Fried, "America's health and health care depend on preventing chronic disease," https://www.huffingtonpost.com/entry/americas-health-and-healthcare-depends-on-preventing_us_58c0649de4b070e55af9eade, March 2017.

[22] P. Trotter, F. Lobelo, and A. Heather, "Chronic disease is healthcare's rising risk," https://www.healthitoutcomes.com/doc/chronic-disease-is-healthcare-s-rising-risk-0001, June 2017.

[23] C. Powell, "Conditional electrical stimulation in animal and human models for neurogenic bladder: working toward a neuroprosthesis," *Current bladder dysfunction reports*, vol. 11, no. 4, pp. 379–385, 2016.

[24] T. M. Bruns, N. Bhadra, and K. J. Gustafson, "Bursting stimulation of proximal urethral afferents improves bladder pressures and voiding," *Journal of neural engineering*, vol. 6, no. 6, p. 066006, 2009.

[25] A. Mendez, M. Sawan, T. Minagawa, and J.-J. Wyndaele, "Estimation of bladder volume from afferent neural activity," *IEEE Transactions on Neural Systems and Rehabilitation Engineering*, vol. 21, no. 5, pp. 704–715, 2013.

[26] J. I. Agbinya, *Principles of Inductive Near Field Communications for Internet of Things*. Wharton, TX, USA: River Publishers, 2011.

[27] M. Masihpour, "Cooperative communication in near field magnetic induction communication systems," Ph.D. dissertation, University of Technology, Sydney, 2012.

[28] N. Jiang, L. Zhang, Z.-Q. Liu, L. Sun, W.-M. Long, P. He, M.-Y. Xiong, and M. Zhao, "Reliability issues of lead-free solder joints in electronic devices," *Science and technology of advanced materials*, vol. 20, no. 1, pp. 876–901, 2019.

[29] P. Si, A. P. Hu, S. Malpas, and D. Budgett, "A frequency control method for regulating wireless power to implantable devices," *IEEE transactions on biomedical circuits and systems*, vol. 2, no. 1, pp. 22–29, 2008.

[30] R. W. Porto, V. J. Brusamarello, L. A. Pereira, and F. R. de Sousa, "Fine tuning of an inductive link through a voltage-controlled capacitance," *IEEE Transactions on Power Electronics*, vol. 32, no. 5, pp. 4115–4124, 2016.

[31] W. Li, G. Wei, C. Cui, X. Zhang, and Q. Zhang, "A double-side self-tuning lcc/s system using a variable switched capacitor based on

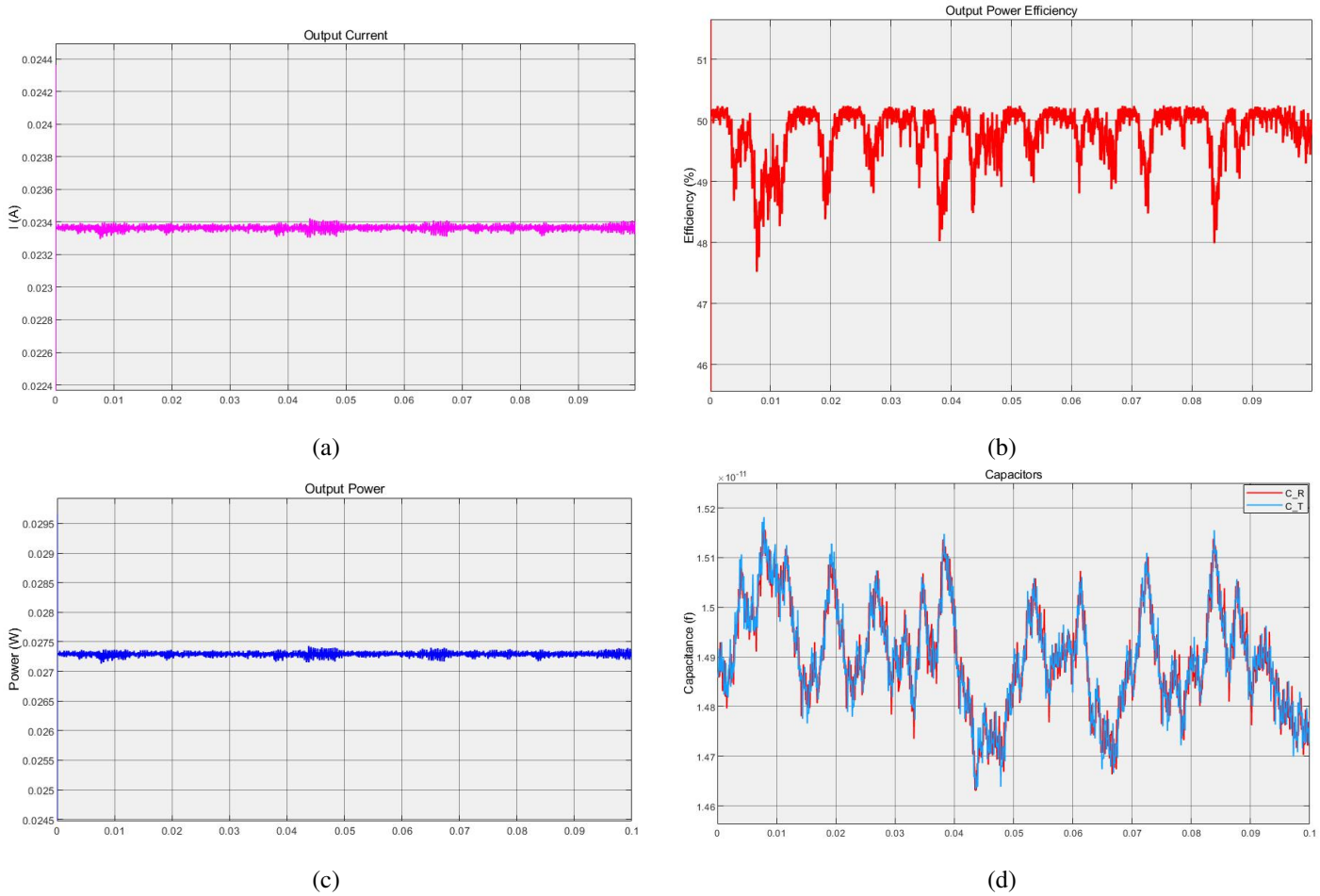


Fig. 8: Second Scenario Controller Performance: a. Output current, b. Efficiency, c. Output power, d. Receiver and transmitter capacitances

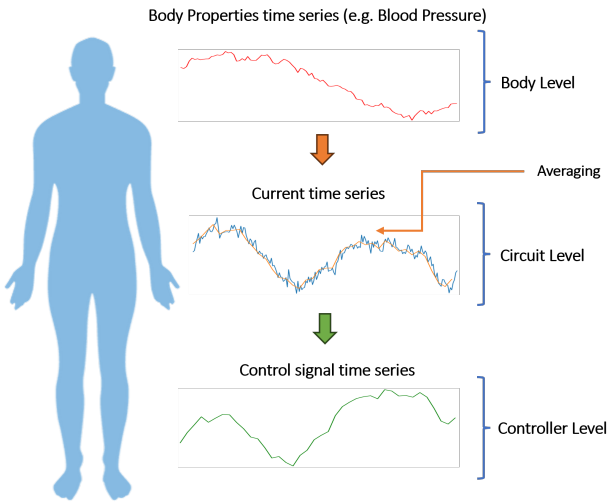


Fig. 9: Circuit in LTspice

parameter recognition," *IEEE Transactions on Industrial Electronics*, vol. 68, no. 4, pp. 3069–3078, 2020.

[32] A. Namadmalan, "Self-oscillating tuning loops for series resonant inductive power transfer systems," *IEEE Transactions on Power Electronics*, vol. 31, no. 10, pp. 7320–7327, 2015.

[33] R. Mai, Y. Liu, Y. Li, P. Yue, G. Cao, and Z. He, "An active-rectifier-based maximum efficiency tracking method using an additional measurement coil for wireless power transfer," *IEEE Transactions on Power Electronics*, vol. 33, no. 1, pp. 716–728, 2017.

[34] J. Van Mulders, D. Delabie, C. Lecluyse, C. Buyle, G. Callebaut, L. Van der Perre, and L. De Strycker, "Wireless power transfer: Systems, circuits, standards, and use cases," *Sensors*, vol. 22, no. 15, p. 5573, 2022.

[35] J. H. Mikkelsen, "Ltspice–an introduction," *Technical report, Institute of Electronic Systems, Aalborg University, Aalborg*, 2005.